# Tuning the Casimir-Lifshitz force with gapped metals

M. Boström,[1,*] M. R. Khan,[1,†] H. R. Gopidi,[1] I. Brevik,[2] Y. Li,[3,4] C. Persson,[5,6] and O. I. Malyi[1,‡]

[1]*Centre of Excellence ENSEMBLE[3] Sp. z o. o., Wolczynska Str. 133, 01-919 Warsaw, Poland*

[2]*Department of Energy and Process Engineering, Norwegian University of Science and Technology, NO-7491 Trondheim, Norway*

[3]*Department of Physics, Nanchang University, Nanchang 330031, China*

[4]*Institute of Space Science and Technology, Nanchang University, Nanchang 330031, China*

[5]*Centre for Materials Science and Nanotechnology, Department of Physics, University of Oslo, P. O. Box 1048 Blindern, NO-0316 Oslo, Norway*

[6]*Department of Materials Science and Engineering, KTH Royal Institute of Technology, SE-100 44 Stockholm, Sweden*

(Received 1 May 2023; revised 5 September 2023; accepted 19 September 2023; published 26 October 2023)

The Casimir-Lifshitz interaction, a long-range force that arises between solids and molecules due to quantum fluctuations in electromagnetic fields, has been widely studied in solid-state physics. The degree of polarization in this interaction is influenced by the dielectric properties of the materials involved, which in turn are determined by factors such as band-to-band transitions, free carrier contributions, phonon contributions, and exciton contributions. Gapped metals, a new class of materials with unique electronic structures, offer the potential to manipulate dielectric properties and, consequently, the Casimir-Lifshitz interaction. In this study, we theoretically investigate the finite temperature Casimir-Lifshitz interaction in $La_3Te_4$-based gapped metal systems with varying off-stoichiometry levels. We demonstrate that off-stoichiometric effects in gapped metals can be used to control the magnitude and, in some cases, even the sign of Casimir-Lifshitz interactions. We predict measurable corrections due to stoichiometry on the predicted Casimir force between a $La_3Te_4$ surface and a gold sphere, attached to an atomic force microscopy tip.

DOI: 10.1103/PhysRevB.108.165306

## I. INTRODUCTION

Solid-state physics textbooks teach us about the Casimir-Lifshitz interaction [1–4], as a long-range force arising between solids and molecules due to quantum fluctuations in the electromagnetic fields [5–7]. This interaction causes the solids or molecules to become polarized when they are close to each other, with the degree of polarization directly influenced by the dielectric properties of the materials [8–23]. This relationship indicates that by manipulating the dielectric properties through external means, it is possible to make an impact on the Casimir-Lifshitz interaction directly. The effects of such manipulations can be directly measured using atomic force microscopy [24] or even be employed in the development of functional devices.

As electronic structure theory has advanced, it has become clear that a material's dielectric properties are determined by several factors: (i) band-to-band transitions between occupied and unoccupied states, which play a significant role across all frequency ranges; (ii) free carrier contributions, typically found in metallic systems at low frequencies; (iii) the phonon contribution; and (iv) exciton contributions, with the latter two primarily limited to the low-frequency range. This understanding implies that by identifying ways to influence factors i-iv, we can effectively tune the dielectric properties of materials and, consequently, the Casimir-Lifshitz interaction. Therefore, the primary challenge lies in discovering materials with tunable dielectric properties.

Recently, gapped metals have emerged as a new class of materials possessing unique electronic structures [25–30]. These compounds set themselves apart from both metals and insulators, as they possess a Fermi level within the principal conduction (or valence) band, resulting in a high intrinsic concentration of free carriers with an internal band gap between their primary band edges. Such materials have attracted significant attention in connection with transparent conductors [28], thermoelectrics [30], and electrides [29]. What makes these materials special is that they can develop off-stoichiometry (within the same parental structure) due to the decay of conducting electrons (holes) to acceptor (donor) states [Figs. 1(a) and 1(b)] formed by intrinsic defect formation [25,31–34]. This is different from the traditional metals and insulators, where defect formation is usually limited to high temperatures and is primarily driven by an increase in configurational entropy [34]. This situation is unique because different off-stoichiometry levels for gapped metals can be achieved, each exhibiting distinct dielectric properties. For example, $La_3Te_4$—an *n*-type gapped metal (i.e., one with its Fermi level in the principal conduction band)—can be experimentally synthesized [35–37] (simply by changing synthesis conditions) across a range of phases from $La_3Te_4$ to $La_{2.67}Te_4$ with their properties tunable from metallic to insulating [31] as schematically shown in Fig. 1(c). Motivated

*mathias.bostrom@ensemble3.eu
†muhammadrizwan.khan@ensemble3.eu
‡oleksandrmalyi@gmail.com

 

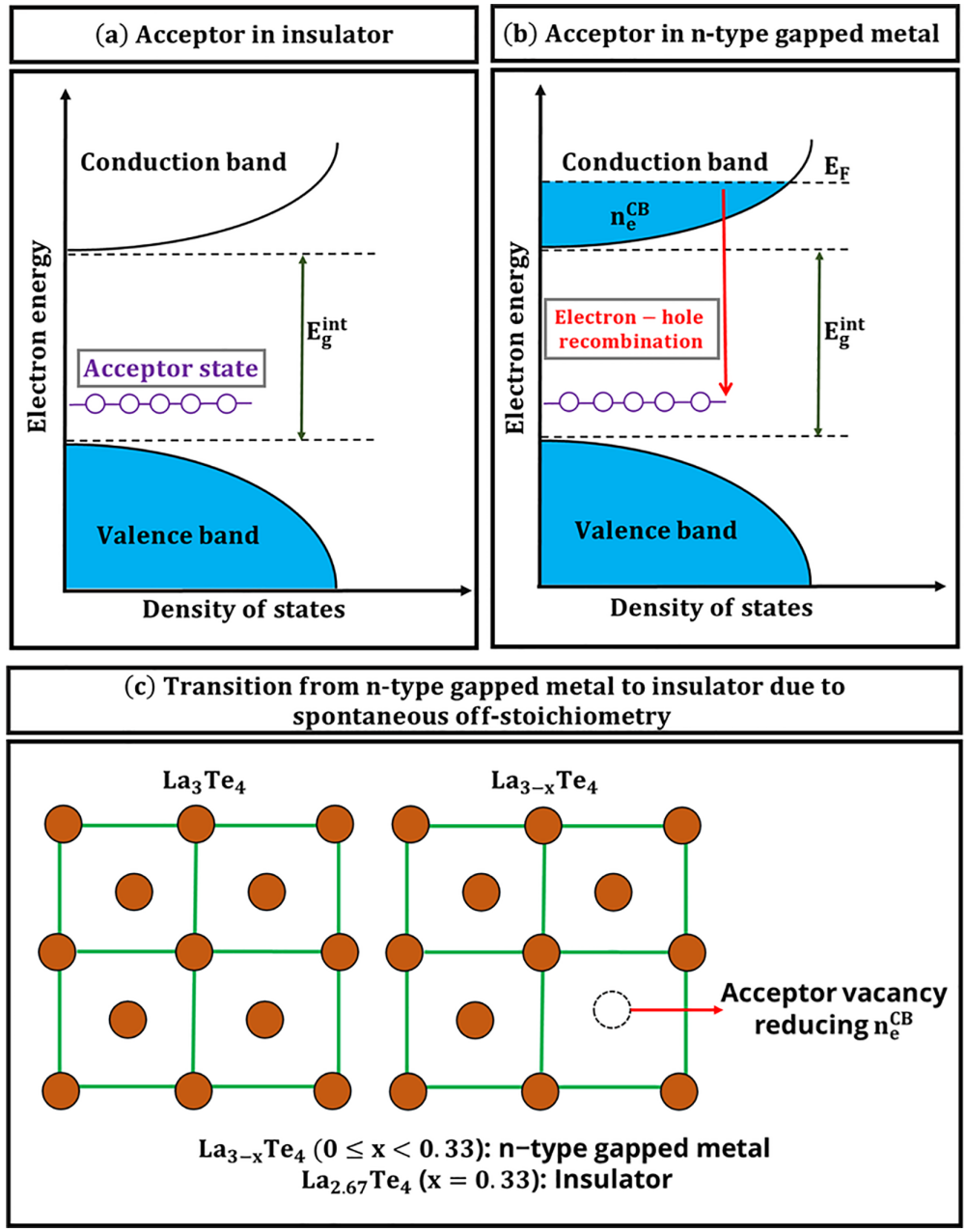


FIG. 1. Origin of off-stoichiometry in $La_3Te_4$ compound. Formation of acceptor vacancy in (a) insulator and (b) *n*-type gapped metal. Here, $E_F$ and $E_g^{int}$ correspond to the Fermi level and internal band gap between the principal valence band maximum and conduction band minimum. (c) Schematic crystal structure for La-Te system depicting metallic state with free electrons in conduction bands and insulator state of $La_{3-x}Te_4$ phase due to presence of acceptor vacancy.

by the above, we study here theoretically the finite temperature Casimir-Lifshitz interaction between different systems involving $La_3Te_4$-based gapped metals, demonstrating how off-stoichiometry can be used as a knob to tune such long-range interaction.

## II. METHODS

### A. Computational details and dielectric functions

To compute the dielectric properties of gapped metals, we perform first-principles calculations using the Perdew-Burke-Ernzerhof exchange-correlation (PBE XC) functional [38] within the VASP framework [39–42]. Our analysis focuses on five distinct $La_{3-x}Te_4$ compounds, previously identified in our earlier work [31]. For each system, we calculate the dielectric properties, considering only the Drude contribution and interband transitions. We employ Γ-centered Monkhorst-Pack *k* grids [43] with 20 000 points per reciprocal atom for the calculations of direct band transitions and plasma frequencies and introduce a subtle Lorentzian broadening of 0.01 eV in the Kramers-Kronig transformation [44]. To include the Drude term in the optical properties, we utilize the kram code [45–47], setting the damping coefficient Γ to 0.2 eV, and additionally investigate the influence of the Γ

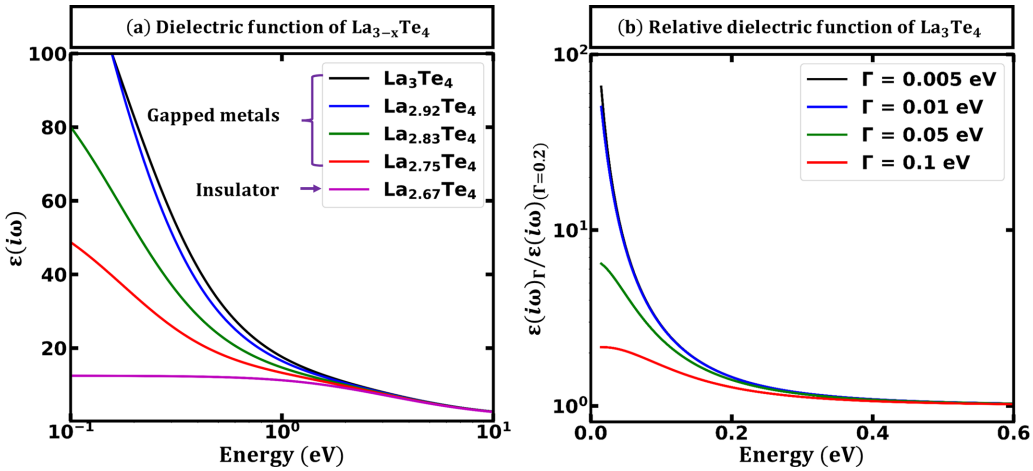


FIG. 2. (a) Dielectric functions for imaginary frequencies from top to bottom for $La_3Te_4$, $La_{2.92}Te_4$, $La_{2.83}Te_4$, $La_{2.75}Te_4$, $La_{2.67}Te_4$. (b) Ratio of the dielectric function for $La_3Te_4$ with different $\Gamma$ (damping coefficient also known as dissipation parameter) to the corresponding values with $La_3Te_4$ with $\Gamma = 0.2$ eV. The results include a superposition of interband transitions and Drude (free electron) contributions, both calculated using DFT.

parameter on our findings. The other details on computational parameters can be found elsewhere [31,48]. Although we are unable to directly compare our calculated dielectric functions with corresponding experimental measurements (no data are available), it is important to highlight that the used methods can describe sufficiently well the experimental trends related to transparency and coloring across a range of gapped metals [25,49].

The quantity related to forces follows from the imaginary ($\varepsilon_i''$) part of the dielectric function

$$\varepsilon_i(i\xi_m) = 1 + \frac{2}{\pi}\int_0^\infty d\omega \frac{\omega\varepsilon_i''(\omega)}{\omega^2 + \xi_m^2}, \quad i = 1, 2, 3, \qquad (1)$$

where the Matsubara frequency is $\xi_m = 2\pi kTm/\hbar$, and the subscript $i$ indicates the medium. As seen in Fig. 2 the curves show strong dependence for the dielectric function on off-stoichiometry for $La_{3-x}Te_4$ (to be specific: $La_3Te_4$ with $E_g^{int} = 1.22$ eV, $La_{2.92}Te_4$ with $E_g^{int} = 1.16 \pm 0.05$ eV, $La_{2.83}Te_4$ with $E_g^{int} = 1.16 \pm 0.05$ eV, $La_{2.75}Te_4$ with $E_g^{int} = 1.16 \pm 0.05$ eV, $La_{2.67}Te_4$ with $E_g^{int} = 1.13$ eV) going from a metallic to insulator behavior. Here, as illustrated in Fig. 1, $E_F$ and $E_g^{int}$ correspond to the Fermi level and internal band gap between the principal valence band maximum and conduction band minimum. In Fig. 2(b), we see for low frequencies the dependence for the dielectric function of $La_3Te_4$ on the $\Gamma$ parameter for $La_3Te_4$. In particular, we present the ratio of the dielectric function for $La_3Te_4$ with different $\Gamma$ to the corresponding values with $La_3Te_4$ with $\Gamma = 0.2$ eV. This highlights that it is only at low frequencies the $\Gamma$ parameter influences the dielectric function. To use the calculated dielectric functions for Casimir-Lifshitz interaction, we also develop the parametrization of the average dielectric function for each of the considered $La_{3-x}Te_4$ systems (Table I) with 14-mode oscillator model [50]

$$\varepsilon(i\xi) = 1 + \sum_j \frac{C_j}{1 + (\xi/\omega_j)^2}, \qquad (2)$$

where $\omega_j$ are characteristic frequencies and $C_j$ are proportional to the oscillator strengths. We note that while all the main parametrization and results for considered $La_{3-x}Te_4$ systems are given for Drude contribution with $\Gamma = 0.2$ eV, below we also provide results for other $\Gamma$ values to verify the role of low Matsubara frequencies on the conclusions of this work.

To describe the Casimir interaction in systems amenable to experimental measurement, we additionally compute the dielectric properties of gold. These calculations are performed using PBEsol [51] XC functional combined with an effective Hubbard correction of $U = 3.0$ eV on the $d$ orbitals according to Dudarev *et al.* [52]. Here, the calculations are performed for 1 atom per primitive cell, the $k$-space summation involved an $80 \times 80 \times 80$ $k$ mesh and a Gaussian smearing of 0.05 eV. The resulting permittivity for gold agrees with the

TABLE I. Parametrization of the average dielectric function of continuous media $\varepsilon(i\xi)$ at imaginary frequencies for $La_{3-x}Te_4$ as calculated with first-principles calculations and a damping coefficient $\Gamma$ set to 0.2 eV. The $\omega_j$ modes are given in eV. The largest difference between fitted and calculated $\varepsilon(i\xi)$ is 0.04%.

| | $C_j$ for different $La_{3-x}Te_4$ compounds | | | | |
|---|---|---|---|---|---|
| Modes ($\omega_j$) | $La_3Te_4$ | $La_{2.92}Te_4$ | $La_{2.83}Te_4$ | $La_{2.75}Te_4$ | $La_{2.67}Te_4$ |
| 0.0203 | 5.6047 | 24.2875 | 0.0 | 0.0 | 0.0 |
| 0.0362 | 15.3667 | 55.9154 | 0.0 | 0.0 | 0.0 |
| 0.0694 | 27.1114 | 98.6417 | 1.2411 | 0.4796 | 0.0008 |
| 0.1325 | 35.8341 | 72.487 | 42.8899 | 19.6292 | 0.0 |
| 0.2085 | 93.1702 | 47.7692 | 42.1523 | 25.6095 | 0.0 |
| 0.4297 | 6.5149 | 7.3256 | 5.479 | 2.4194 | 0.0095 |
| 0.8328 | 2.9159 | 1.447 | 0.7619 | 0.4956 | 0.0421 |
| 1.9083 | 2.4749 | 2.9666 | 3.022 | 3.3971 | 3.1313 |
| 3.2388 | 4.6107 | 4.3332 | 4.464 | 4.5286 | 4.8426 |
| 5.2955 | 2.7231 | 2.8949 | 2.7872 | 2.6545 | 2.4639 |
| 8.9753 | 0.7087 | 0.5961 | 0.6287 | 0.6727 | 0.7464 |
| 18.2815 | 0.1959 | 0.2782 | 0.2486 | 0.205 | 0.1581 |
| 23.0355 | 0.0695 | 0.0069 | 0.022 | 0.0474 | 0.0716 |
| 42.0922 | 0.0 | 0.0057 | 0.0042 | 0.0018 | 0.0 |

experimental data presented in Ref. [53]. The plasma frequency was calculated to 9.6 eV and we used that with $\Gamma = 0.05$ eV when calculating the Drude contribution.

### B. Theory of the Casimir force

Let $F(L)$ be the free energy per unit surface area between planar surfaces, and $f(L)$ be the force between a gapped metal (medium 1) and a sphere with radius $R$ (medium 3). For $L \ll R$ the force between a sphere and a planar surface can be deduced from the free energy between two planar surfaces using the so-called proximity force approximation [4]. The sphere may be gold, a gapped transparent conductor, or an air bubble. The intervening medium 2 may be a diluted gas with $\varepsilon_2(i\xi_m) \sim 1$, or water with dielectric functions given in the literature [54,55]. The free energy and force can be written as [2,4]

$$F(L) = \frac{f(L)}{2\pi R} = \frac{k_B T}{2\pi} {\sum_{m=0}^{\infty}}' \int_0^\infty dq\, q \sum_\sigma \ln\left(1 - r_\sigma^{21} r_\sigma^{23} \mathrm{e}^{-2\kappa_2 L}\right), \tag{3}$$

where $\sigma = \mathrm{TE}, \mathrm{TM}$, and the prime in the sum above indicates that the first term $m = 0$ has to be weighted by $1/2$. The Fresnel reflection coefficients between surfaces $i$ and $j$ for the transverse magnetic (TM) and transverse electric (TE) polarizations are given by

$$r_{\mathrm{TE}}^{ij} = \frac{\kappa_i - \kappa_j}{\kappa_i + \kappa_j}; \quad r_{\mathrm{TM}}^{ij} = \frac{\varepsilon_j \kappa_i - \varepsilon_i \kappa_j}{\varepsilon_j \kappa_i + \varepsilon_i \kappa_j}. \tag{4}$$

Here $\kappa_i = \sqrt{q^2 + \varepsilon_i \xi_m^2/c^2}$, with $i = 1, 2, 3$ and the Matsubara frequency is defined above. Notably, since the dielectric constant is finite for gapped metals unless we set $\Gamma = 0$, the transverse electric reflection coefficient between nonmagnetic gapped metals and dilute gas goes to zero ($r_{\mathrm{TE}}^{21} = 0 \quad as \quad \xi \to 0$). As a comparison, we also consider what happens when we assume perfect metallic behavior for the transverse electric reflection coefficients in the zero-frequency limit [11,13,22] ($r_{\mathrm{TE}}^{21} r_{\mathrm{TE}}^{23} = 1 \quad as \quad \xi \to 0$). The alternative limiting behavior leads to the "perfect metal correction" (PMC) to the interaction between real metal surfaces (when $L \ll R$) [11,13,22]

$$\Delta F^{\mathrm{PMC}}(L) = \frac{\Delta f^{\mathrm{PMC}}(L)}{2\pi R} = \frac{-k_B T \zeta(3)}{16\pi L^2}, \tag{5}$$

where $\zeta(x)$ is the Riemann zeta function. This could be the case if the dielectric function for $La_3Te_4$ is not finite as $\xi \to 0$, and goes to infinite at least as $1/\xi^2$. The energy correction factor $\eta(L, T)$ is defined [4] as the ratio of the calculated Casimir force and the corresponding Casimir force between a perfectly conducting sphere with radius $R$ and a perfectly conducting plane (when $L \ll R$) at zero temperature [5]:

$$F_C(L) = \frac{f_C(L)}{2\pi R} \cong \frac{-\pi^2 \hbar c}{720 L^3}, \tag{6}$$

$$\eta(L, T) = \frac{f(L)}{f_C(L)} = \frac{F(L)}{F_C(L)}. \tag{7}$$

We will match our results against an ideal case (relevant to any metal surfaces behaving as ideal plasmas [2]). For two metallic surfaces interacting across air, it is thus relevant for comparison to include the "perfect metal correction" by adding Eq. (5) and Eq. (3) and divide the sum with Eq. (6). The corrected ratio is

$$\eta^* = \frac{f(L) + \Delta f^{\mathrm{PMC}}(L)}{f_C(L)} = \frac{F(L) + \Delta F^{\mathrm{PMC}}(L)}{F_C(L)}. \tag{8}$$

### C. A note on the effect of dissipation

The dissipation is included in our paper via a damping term $\Gamma$ in the Drude dispersion relation, thus not from microscopic models. To see this from a broader perspective, it may be worthwhile to start from the general case where the temperature dependence of $\Gamma$ is also taken into account. We have then

$$\varepsilon(i\xi, T) = 1 + \frac{\omega_{pl}^2}{\xi[\xi + \Gamma(T)]}, \tag{9}$$

where $\xi$ is the imaginary frequency. If one at first ignores impurities, one may here make use of the Bloch-Grüneisen formula [56] for the temperature variation of the electrical resistivity $\rho$, the latter being proportional to $\Gamma$. This formula implies, among other things, that $\varepsilon(i\xi, T)$ is actually higher when $T$ is low than at room temperature if the frequencies are lower than about $10^{14}$ rad/s, i.e., of the same order as the first Matsubara frequency at room temperature (cf. the discussion on these points by Høye *et al.* [57,58]). Now, from numerical estimates, it turns out that the influence of the temperature on $\Gamma$ is modest. A more important factor in this context is the presence of impurities in the metal. The existence of these makes the resistivity $\rho$, and thus also $\Gamma$, constant at low temperatures and low frequencies. Consequently, we can put $\varepsilon(i\xi, T) \to \varepsilon(i\xi) \propto 1/\xi$ when $\xi \to 0$. Now one must recognize that for practical purposes it is not $\varepsilon$ itself that is the central quantity, but rather the combination

$$\xi^2[\varepsilon(i\xi) - 1], \tag{10}$$

which has to go to zero as $\xi \to 0$. This relationship is satisfied by the simple Drude ansatz for the dispersion equation, and the Casimir theory for metals becomes consistent. The expression Eq. (10) implies that the contribution to the Casimir force from the TE zero mode vanishes, and also that the Nernst theorem becomes satisfied (i.e., that the free energy depicted as a function of $T$ has a zero slope as $T \to 0$). Cf. again the mentioned references by Høye *et al.* [57,58].

## III. RESULTS

### A. A pair of identical $La_{3-x}Te_4$ surfaces

To demonstrate the effect of off-stoichiometry on the Casimir-Lifshitz force, we first consider the interaction between a pair of identical gapped metal planar surfaces interacting across the air as a function of interplane distance [Fig. 3(a)]. At short separations, that is, when the finite velocity of light can be approximated as infinite, the product of reflection coefficients [*c.f.* Eq. (3) and Eq. (4)] goes as [4]

$$\frac{(\varepsilon_1 - \varepsilon_2)^2}{(\varepsilon_1 + \varepsilon_2)^2}. \tag{11}$$

From this part of the full expression Eq. (3), two things can be deduced: (i) the force between identical surfaces is attractive,

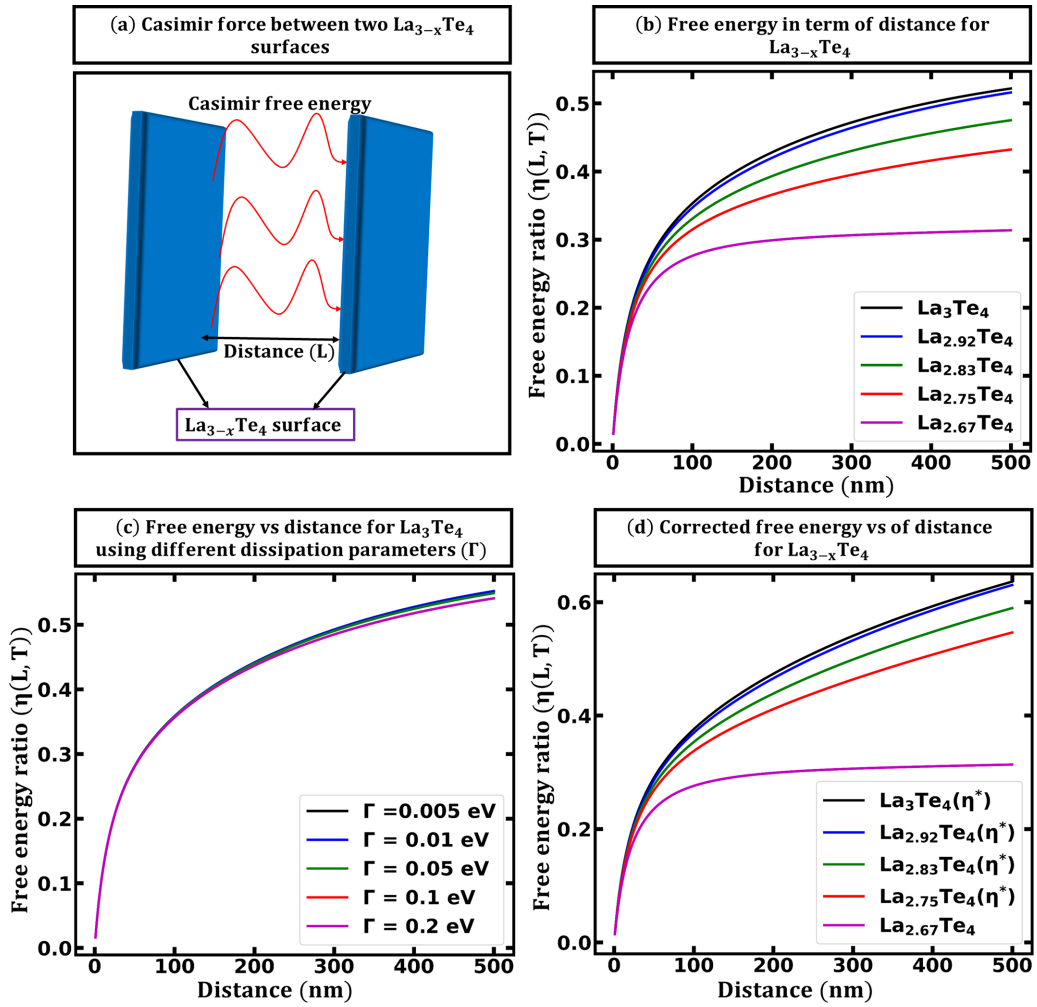


FIG. 3. (a) Schematic scheme over the setup. (b) Energy correction factor $\eta(L, T)$ between equal-gapped metal surfaces across air at T = 300 K. (c) $\eta(L, T)$ for two equal $La_{3-x}Te_4$ varying the Γ. (d) Same as in (b) but adding the "perfect metal correction" to the free energy for the metallic systems. The Drude damping parameter is here introduced on a phenomenological level. The influence from dissipation does not significantly change the strength of the interaction. In Fig. 3(d), the reported change is however different, since it arises from the "perfect metal correction." The limiting value in the case with $\eta^*$ ($\varepsilon \to 1/\omega^2$) refers to the slowest possible decay in the low-frequency limit (i.e., not the actual zero-frequency limit) in which the zero-frequency TE mode would be expected to contribute.

and (ii) the closer the ratio in Eq. (11) is to 1 (i.e., the more metallic), the stronger the attraction.

The Casimir-Lifshitz free energy between gapped metal surfaces at finite temperatures is predicted to deviate strongly from the T = 0 K ideal metal Casimir interaction. (Note that the long-range thermal asymptote decays slower than the zero-temperature Casimir asymptote, leading to an increase of the ratio with increasing separations). As can be seen in Figs. 3(b)–3(d), off-stoichiometry effects for gapped metals can be used as an effective knob to induce 10–40% changes in the magnitude of the interaction. Notably, in the separation range where forces are typically measured, the effects are of the same magnitude as any potential corrections from "the ideal metal" (plasma model) plate zero-frequency transverse electric contribution. The force in Fig. 3(b) increases in magnitude as the surfaces become more metallic (up to a limit where the product of the reflection coefficient in a specific frequency range is close to one). The results shown in Fig. 3(d) is the corresponding case when the ideal metal or "plasma model" approximation [2] is used for the zero-frequency term.

Another important observation is that interaction between different metallic $La_{3-x}Te_4$ surfaces is also different (i.e., dependent on $x$). This behavior can be understood on the electronic structure theory level as increasing the off-stoichiometry results in a change of free carrier concentration (each La vacancy removes three electrons from the principal conduction band), reducing the free carrier contribution to $\varepsilon(i\xi)$. Hence, even though multiple $La_{3-x}Te_4$ surfaces are metallic, they substantially differ in dielectric functions simply due to differences in free carrier concentration.

As noted above, the dielectric properties of materials are defined by the superposition of different contributions. While one can explicitly calculate the band-to-band transition, the calculation of free carrier contribution to dielectric function relies on the Drude model. We described in Fig. 2 the effect on the low-frequency tail of the dielectric function from changes

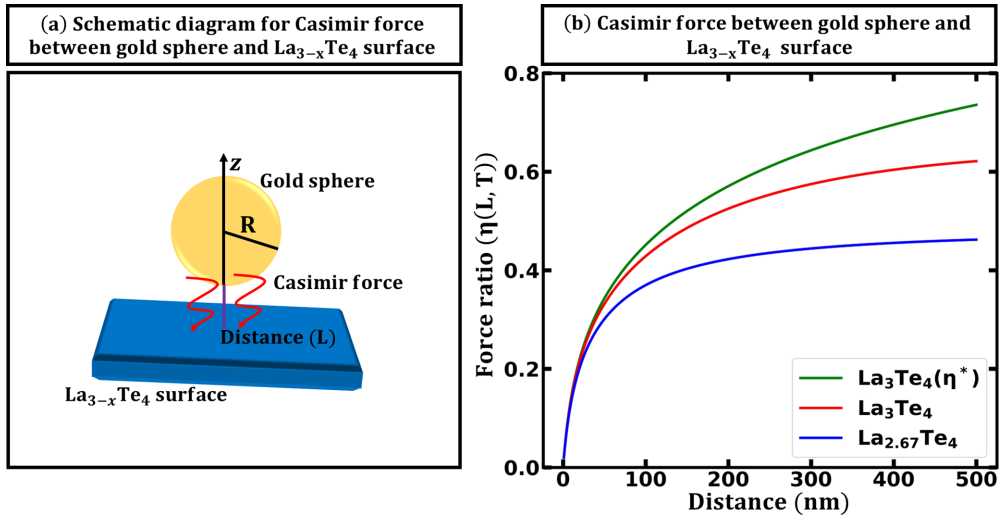


FIG. 4. Schematic setup and the $\eta(L, T) = f(L)/f_C$ at T = 300 K for a gold sphere interacting with (i) $La_3Te_4$, (ii) $La_3Te_4$ with PMC, i.e., $\xi = 0$ transverse electric "Perfect Metal Correction," or (iii) $La_{2.67}Te_4$ surface. The limiting value in the case with $\eta^*$ ($\varepsilon \to 1/\omega^2$) refers to the slowest possible decay in the low-frequency limit (i.e., not the actual zero-frequency limit) in which the zero-frequency TE mode would be expected to contribute.

in the choice of damping coefficient in the Drude model ($\Gamma$). The static dielectric constant rises to higher values with a reduced $\Gamma$. However, in Fig. 3(c), we show how slight the energy correction factor is on the choice of damping coefficient for the specific case of a pair of $La_3Te_4$ surfaces. Since the gapped metal surfaces have large but finite dielectric constants, one would expect the "perfect metal correction" to be purely hypothetical. However, future optical and force measurements will enable us to distinguish better how to accurately model the dielectric functions at extremely low frequencies.

### B. Gold sphere in air near $La_{3-x}Te_4$ surfaces

As is well known, all ordinary metals have a finite static conductivity. The Drude model describes the optical and dielectric properties quite well for small frequencies. The dielectric function in the Drude model is

$$\varepsilon(\omega) = 1 + \frac{i\sigma(\omega)}{\omega} = 1 - \frac{\omega_{pl}^2}{\omega(\omega + i\Gamma)}. \tag{12}$$

Setting the damping parameter $\Gamma$ zero, the plasma model is obtained. The damping parameter has a real physical origin, and is the result of scattering of the carriers against lattice imperfections. At finite temperature, processes with phonons emitted or absorbed further contribute. Boström and Sernelius [11,13] found that the damping parameter has a dramatic effect on the Casimir interaction between gold surfaces at separations where the finite temperature is important. The plasma model actually predicts a result that coincides with that of the classic Casimir gedanken experiment between two perfectly reflecting half-spaces, while the Drude model predicts that this result is reduced by a factor of two. In the limit of large $L \to \infty$ (while still demanding $\frac{L}{R} \ll 1$), the ratio for two interacting metallic surfaces would, within the PMC, become asymptotically

$$\eta^* \sim \frac{90 L k_B T \zeta(3)}{\pi^3 \hbar c}, \tag{13}$$

while $\eta$ in the same limit has half this magnitude. For all cases considered, the ratios go (for large $L$) $\propto Lk_BT/(\hbar c)$. This means, as is well known, that the ratio increases linearly with separation for large $L$. Some experiments favor the Drude model [10,16,19] while most appear to favor the plasma model [2,17,18,22]. The materials we consider are evaluated by density-functional theory to have large, but finite, values for the zero-frequency permittivity (but should go to infinity if $\Gamma \to 0$). They should hence have a free-energy behavior not observed experimentally by, for example, Mohideen and collaborators for metal surfaces [2,17,18,22]. Rather it is expected to be closer to the experimental observations by Lamoreaux and his collaborators [10,16,19] (and even more to the case of doped silicon surfaces). If future experiments would prove this to be wrong, further research must be prompted into how to model the low-frequency part of the dielectric functions for gapped metals within density-functional theory.

Typically, experimental measurements of Casimir forces are conducted using atomic-force microscopy (AFM), where a specialized sphere (e.g., Au) is attached to the AFM tip. Because of this, herein we also consider another proposed experimental setup shown in Fig. 4, where we consider Au sphere attached to an atomic force microscope tip, interacting with a planar surface of different $La_{3-x}Te_4$ surfaces at different separation. We present our result in terms of the ratio between the calculated force and the corresponding hypothetical force between a perfectly conducting plane and a perfectly conducting sphere (in the limit of zero temperature). Very similar systems, but with different material combinations, have been carefully studied by some of the world's best groups in force measurements. Notably, as we clearly demonstrate, both off-stoichiometry and "perfect metal correction" effects are large enough to be within the few percentage measurement accuracy claimed in the 0.1 μm range in several experimental labs (for instance by Mohideen and coworkers) [10,17,19,22,59–62].

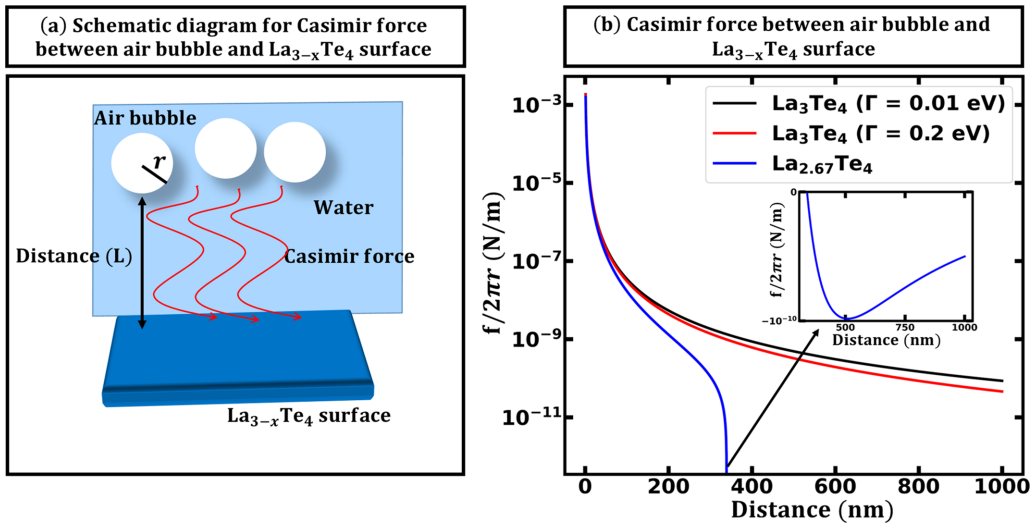


FIG. 5. Casimir force at T = 273.16 K between an air bubble in cold water [55] near (i) $La_3Te_4$ with $\Gamma = 0.2$ eV, (ii) $La_3Te_4$ with $\Gamma = 0.01$ eV, and (iii) $La_{2.67}Te_4$. The sizes of the bubbles vary depending on the system involved from nanobubbles, micron-sized bubbles to millibubbles.

### C. Air bubble in liquid water near $La_{3-x}Te_4$ surfaces

One interesting prediction from theory and force measurements is that these forces can be repulsive [6,8,9,63–68], and even change sign [69,70]. When reflecting on the expression for the Casimir-Lifshitz interaction, it is clear that repulsion occurs whenever $\varepsilon_1 > \varepsilon_2 > \varepsilon_3$ for a broad range of finite Matsubara frequencies. This was well known to Dzyaloshinskii, Lifshitz, and Pitaevskii [6]. A remarkable point discussed by Elbaum and Schick [69] is that the dispersion forces (including [4], e.g., van der Waals, Casimir-Polder, Lifshitz, and Casimir interactions) can change sign when for a range of "high" frequencies (small separations) $\varepsilon_1 > \varepsilon_2 > \varepsilon_3$, while for low frequencies (large separations) $\varepsilon_2 > \varepsilon_1 > \varepsilon_3$. The origin of this effect is the relevant reflection coefficients combined with the exponential factor $e^{-2\sqrt{q^2+\varepsilon_2\xi_m^2/c^2}L}$. At very large separations [the factor $\sqrt{\varepsilon_2}L\xi_m/(qc)$ should be small or of the order unity to result in a significant contribution to the interaction], the finite velocity of light means only the zero-frequency term contributes. If $\varepsilon_2(0) > \varepsilon_1(0) > \varepsilon_3(0)$, then long-range attraction follows.

We demonstrate in Fig. 5 that the Casimir-Lifshitz force between an air bubble in water near a gapped metal surface can, via control of the off-stoichiometry and separation, at large separations change from repulsion to attraction. We propose that further studies on how to tune more effectively the transition from repulsion to attraction-based trapping of gas bubbles in liquids must include other effects including hydration, dissolved gases, surface charges, and ion-specific double-layer forces within the Derjaguin-Landau-Verwey-Overbeek (DLVO) theory and beyond [3,71].

## IV. CONCLUSIONS

As dimensions and distances relevant for nanomachines go down in size, it becomes increasingly important to control the sign and magnitude of short-range van der Waals/Casimir-Lifshitz interactions [66,72,73] and torques [74,75]. We observe that in the literature one finds that similar analyses have been performed for conductive oxides, phase-changing materials, chiral materials, magnetic material, Weyl semimetals, graphene, topological insulators, and many other systems. We refer the readers to the review by Woods and collaborators [76]. Herein, we investigate the effects of off-stoichiometry on the Casimir-Lifshitz force between $La_{3-x}Te_4$ surfaces in various experimental setups. The results show that off-stoichiometry affects significantly impact the interaction between different $La_{3-x}Te_4$ surfaces. In particular, we propose that these forces can be influenced to more than 10–40% by manipulating the off-stoichiometry of gapped metal and tuning it from metallic to insulating behavior (this phenomenon is due to the fact that $La_3Te_4$-gapped metal possesses a distinctive electronic structure resulting in the reduction of free carrier concentration by the formation of La vacancies). The study of this new material category indicates a roadmap for how to enhance or reduce Casimir-Lifshitz interactions. As we show, for gas bubbles in liquid water near a gapped metal, tuning off-stoichiometry effects can even change the sign of the long-range part of the Casimir-Lifshitz interactions. Our main conclusion is that off-stoichiometry in gapped metals can be used as a knob to tune long-range interactions. In a longer perspective, the use of controlled quantum switches for fluid systems, together with an exploitation of off-stoichiometry effects, may be a promising way to investigate the Drude/plasma controversy.

## ACKNOWLEDGMENTS

The authors thank the "ENSEMBLE3—Center of Excellence for nanophotonics, advanced materials, and novel crystal growth-based technologies" project (Grant No. MAB/2020/14) carried out within the International Research Agendas program of the Foundation for Polish Science cofinanced by the European Union under the European Regional Development Fund, the European Union's Horizon

2020 research and innovation program Teaming for Excellence (Grant No. 857543), and European Union's Horizon 2020 research and innovation programme (Grant No. 101058694), for support of this work. We gratefully acknowledge Poland's high-performance computing infrastructure PLGrid (HPC Centers: ACK Cyfronet AGH) for providing computer facilities and support within computational Grant No. PLG/2023/016228 and for awarding access to the LUMI supercomputer, owned by the EuroHPC Joint Undertaking, hosted by CSC (Finland) and the LUMI consortium through Grant No. PLL/2023/04/016500. We also acknowledge access to high-performance computing resources via NAISS, provided by NSC and PDC, as well as NOTUR, provided by Sigma2.

[1] K. A. Milton, *The Casimir Effect: Physical Manifestations of Zero-Point Energy* (World Scientific, River Edge, USA, 2001).
[2] M. Bordag, G. L. Klimchitskaya, U. Mohideen, and V. M. Mostepanenko, *Advances in the Casimir Effect* (Oxford Science Publications, Oxford, 2009).
[3] B. W Ninham and P. Lo Nostro, *Molecular Forces and Self Assembly in Colloid, Nano Sciences and Biology*, Cambridge Molecular Science (Cambridge University Press, Cambridge, 2010).
[4] Bo E. Sernelius, *Fundamentals of van der Waals and Casimir Interactions*, Springer Series on Atomic, Optical, and Plasma Physics (Springer International Publishing, Switzerland, 2018).
[5] H. B. G. Casimir, On the attraction between two perfectly conducting plates, in *Proceedings of the KNAW*, Vol. 51 (1948), pp. 793–795.
[6] I. E. Dzyaloshinskii, E. M. Lifshitz, and L. P. Pitaevskii, The general theory of van der Waals forces, Adv. Phys. **10**, 165 (1961).
[7] V. A. Parsegian and B. W. Ninham, Application of the Lifshitz theory to the calculation of Van der Waals forces across thin lipid films, Nature (London) **224**, 1197 (1969).
[8] P. Richmond and B. W. Ninham, Calculations, using Lifshitz theory, of the height vs. thickness for vertical liquid helium films, Solid State Commun. **9**, 1045 (1971).
[9] P. Richmond, B. W. Ninham, and R. H. Ottewill, A theoretical study of hydrocarbon adsorption on water surfaces using Lifshitz theory, J. Colloid Interface Sci. **45**, 69 (1973).
[10] S. K. Lamoreaux, Demonstration of the Casimir force in the 0.6 to 6 μ m range, Phys. Rev. Lett. **78**, 5 (1997).
[11] M. Boström and Bo E. Sernelius, Thermal effects on the Casimir force in the 0.1−5 μ m range, Phys. Rev. Lett. **84**, 4757 (2000).
[12] M. Bordag, B. Geyer, G. L. Klimchitskaya, and V. M. Mostepanenko, Casimir force at both nonzero temperature and finite conductivity, Phys. Rev. Lett. **85**, 503 (2000).
[13] Bo E. Sernelius and M. Boström, Comment on 'Casimir force at both nonzero temperature and finite conductivity', Phys. Rev. Lett. **87**, 259101 (2001).
[14] M. Boström and B. E. Sernelius, Entropy of the Casimir effect between real metal plates, Phys. A: Stat. **339**, 53 (2004).
[15] K. A. Milton, The Casimir effect: Recent controversies and progress, J. Phys. A: Math. Gen. **37**, R209 (2004).
[16] S. K. Lamoreaux, The Casimir force: Background, experiments, and applications, Rep. Prog. Phys. **68**, 201 (2005).
[17] C.-C. Chang, A. A. Banishev, R. Castillo-Garza, G. L. Klimchitskaya, V. M. Mostepanenko, and U. Mohideen, Gradient of the Casimir force between Au surfaces of a sphere and a plate measured using an atomic force microscope in a frequency-shift technique, Phys. Rev. B **85**, 165443 (2012).
[18] G. L. Klimchitskaya, U. Mohideen, and V. M. Mostepanenko, The Casimir force between real materials: Experiment and theory, Rev. Mod. Phys. **81**, 1827 (2009).
[19] A. O. Sushkov, W. J. Kim, D. A. R. Dalvit, and S. K. Lamoreaux, Observation of the thermal Casimir force, Nat. Phys. **7**, 230 (2011).
[20] M. Boström, M. Dou, O. I. Malyi, P. Parashar, D. F. Parsons, I. Brevik, and C. Persson, Fluid-sensitive nanoscale switching with quantum levitation controlled by $\alpha$-Sn/$\beta$-Sn phase transition, Phys. Rev. B **97**, 125421 (2018).
[21] V. Esteso, S. Carretero-Palacios, and H. Míguez, Casimir-Lifshitz force based optical resonators, J. Phys. Chem. Lett. **10**, 5856 (2019).
[22] G. L. Klimchitskaya, U. Mohideen, and V. M. Mostepanenko, The Casimir effect in graphene systems: Experiment and theory, Int. J. Mod. Phys. A **37**, 2241003 (2022).
[23] V. V. Nesterenko, Plasma model and Drude model permittivities in Lifshitz formula, Eur. Phys. J. C **82**, 874 (2022).
[24] W. Ducker, T. Senden, and R. Pashley, Direct measurement of colloidal forces using an atomic force microscope, Nature (London) **353**, 239 (1991).
[25] O. I. Malyi, M. T. Yeung, K. R. Poeppelmeier, C. Persson, and A. Zunger, Spontaneous non-stoichiometry and ordering in degenerate but gapped transparent conductors, Matter **1**, 280 (2019).
[26] X. Zhang, L. Zhang, J. D. Perkins, and A. Zunger, Intrinsic transparent conductors without doping, Phys. Rev. Lett. **115**, 176602 (2015).
[27] F. Ricci, A. Dunn, A. Jain, G.-M. Rignanese, and G. Hautier, Gapped metals as thermoelectric materials revealed by high-throughput screening, J. Mater. Chem. A **8**, 17579 (2020).
[28] L. Zhang, Y. Zhou, L. Guo, W. Zhao, A. Barnes, H.-T. Zhang, C. Eaton, Y. Zheng, M. Brahlek H. F. Haneef *et al.*, Correlated metals as transparent conductors, Nat. Mater. **15**, 204 (2016).
[29] S. Matsuishi, Y. Toda, M. Miyakawa, K. Hayashi, T. Kamiya, M. Hirano, I. Tanaka, and H. Hosono, High-density electron anions in a nanoporous single crystal: $[Ca_{24}Al_{28}O_{64}]^{4+}(4e^-)$, Science **301**, 626 (2003).
[30] A. F. May, J.-P. Fleurial, and G. J. Snyder, Thermoelectric performance of lanthanum telluride produced via mechanical alloying, Phys. Rev. B **78**, 125205 (2008).
[31] M. R. Khan, H. R. Gopidi, M. Wlazlo, and O. I. Malyi, Fermi-level instability as a way to tailor the properties of $La_{3-x}Te_4$, J. Phys. Chem. Lett. **14**, 1962 (2023).
[32] O. I. Malyi and A. Zunger, False metals, real insulators, and degenerate gapped metals, Appl. Phys. Rev. **7**, 041310 (2020).
[33] O. I. Malyi, G. M. Dalpian, X.-G. Zhao, Z. Wang, and A. Zunger, Realization of predicted exotic materials: The burden of proof, Mater. Today **32**, 35 (2020).

[34] A. Zunger and O. I. Malyi, Understanding doping of quantum materials, Chem. Rev. **121**, 3031 (2021).

[35] T. H. Ramsey, H. Steinfink, and E. J. Weiss, The phase equilibria and crystal chemistry of the rare earth-group VI systems. IV. Lanthanum-Tellurium, Inorg. Chem. **4**, 1154 (1965).

[36] O. Delaire, A. F. May, M. A. McGuire, W. D. Porter, M. S. Lucas, M. B. Stone, D. L. Abernathy, V. A. Ravi, S. A. Firdosy, and G. J. Snyder, Phonon density of states and heat capacity of $La_{3-x}Te_4$, Phys. Rev. B **80**, 184302 (2009).

[37] J. Li, R. Liu, Q. Song, Z. Gao, H. Huang, Q. Zhang, X. Shi, S. Bai, and L. Chen, Enhanced thermal stability and oxidation resistance in $La_{3-x}Te_4$ by compositing metallic nickel particles, Acta Mater. **224**, 117526 (2022).

[38] J. P. Perdew, K. Burke, and M. Ernzerhof, Generalized gradient approximation made simple, Phys. Rev. Lett. **77**, 3865 (1996).

[39] G. Kresse and J. Hafner, *Ab Initio* molecular dynamics for liquid metals, Phys. Rev. B **47**, 558 (1993).

[40] G. Kresse and J. Furthmüller, Efficiency of *ab-initio* total energy calculations for metals and semiconductors using a plane-wave basis set, Comput. Mater. Sci. **6**, 15 (1996).

[41] G. Kresse and J. Furthmüller, Efficient iterative schemes for *ab initio* total-energy calculations using a plane-wave basis set, Phys. Rev. B **54**, 11169 (1996).

[42] G. Kresse and D. Joubert, From ultrasoft pseudopotentials to the projector augmented-wave method, Phys. Rev. B **59**, 1758 (1999).

[43] H. J. Monkhorst and J. D. Pack, Special points for brillouin-zone integrations, Phys. Rev. B **13**, 5188 (1976).

[44] L. D. Landau and E. M. Lifshitz, *Statistical Physics*, 3rd ed., Vol. 5 (Oxford University Press, Oxford, 1980).

[45] P. Blaha, K. Schwarz, F. Tran, R. Laskowski, G. K. H. Madsen, and L. D. Marks, WIEN2k: An APW+ lo program for calculating the properties of solids, J. Chem. Phys. **152**, 074101 (2020).

[46] P. Blaha, K. Schwarz, P. Sorantin, and S. B. Trickey, Full-potential, linearized augmented plane wave programs for crystalline systems, Comput. Phys. Commun. **59**, 399 (1990).

[47] P. Blaha, K. Schwarz, G. K. H. Madsen, D. Kvasnicka, J. Luitz, R. Laskowski, F. Tran, and L. D. Marks, WIEN2k, *An Augmented Plane Wave + Local Orbitals Program for Calculating Crystal Properties* (Vienna University of Technology, Austria, Karlheinz Schwarz, 2018).

[48] M. R. Khan, H. R. Gopidi, H. R. Darabian, D. A. Pawlak, and O. I. Malyi, Spontaneous off-stoichiometry as the knob to control dielectric properties of gapped metals, Phys. Chem. Chem. Phys. **25**, 20287 (2023).

[49] M. R. Khan, H. R. Gopidi, and O. I. Malyi, Optical properties and electronic structures of intrinsic gapped metals: Inverse materials design principles for transparent conductors, Appl. Phys. Lett. **123**, 061101 (2023).

[50] O. I. Malyi, M. Boström, V. V. Kulish, P. Thiyam, D. F. Parsons, and C. Persson, Volume dependence of the dielectric properties of amorphous $SiO_2$, Phys. Chem. Chem. Phys. **18**, 7483 (2016).

[51] J. P. Perdew, A. Ruzsinszky, G. I. Csonka, O. A. Vydrov, G. E. Scuseria, L. A. Constantin, X. Zhou, and Burke K., Restoring the density-gradient expansion for exchange in solids and surfaces, Phys. Rev. Lett. **100**, 136406 (2008).

[52] S. L. Dudarev, G. A. Botton, S. Y. Savrasov, C. J. Humphreys, and A. P. Sutton, Electron-energy-loss spectra and the structural stability of nickel oxide: An LSDA+U study, Phys. Rev. B **57**, 1505 (1998).

[53] I. Zorić, M. Zäch, B. Kasemo, and C. Langhammer, Gold, platinum, and aluminum nanodisk plasmons: Material independence, subradiance, and damping mechanisms, ACS Nano **5**, 2535 (2011).

[54] J. Fiedler, M. Boström, C. Persson, I. H. Brevik, R. W. Corkery, S. Y. Buhmann, and D. F. Parsons, Full-spectrum high resolution modeling of the dielectric function of water, J. Phys. Chem. B **124**, 3103 (2020).

[55] J. Luengo-Marquez, F. Izquierdo-Ruiz, and L. G. MacDowell, Intermolecular forces at ice and water interfaces: Premelting, surface freezing, and regelation, J. Chem. Phys. **157**, 044704 (2022).

[56] D. E. Gray (ed.), *Handbook of Physics* (McGraw-Hill, New York, 1972).

[57] J. S. Høye, I. Brevik, J. B. Aarseth, and K. A. Milton, Does the transverse electric zero mode contribute to the Casimir effect for a metal? Phys. Rev. E **67**, 056116 (2003).

[58] I. Brevik, J. B. Aarseth, J. S. Høye, and K. A. Milton, Temperature dependence of the Casimir effect, Phys. Rev. E **71**, 056101 (2005).

[59] B. W. Harris, F. Chen, and U. Mohideen, Precision measurement of the Casimir force using gold surfaces, Phys. Rev. A **62**, 052109 (2000).

[60] R. S. Decca, D. López, E. Fischbach, and D. E. Krause, Measurement of the Casimir force between dissimilar metals, Phys. Rev. Lett. **91**, 050402 (2003).

[61] A. Le Cunuder, A. Petrosyan, G. Palasantzas, V. Svetovoy, and S. Ciliberto, Measurement of the Casimir force in a gas and in a liquid, Phys. Rev. B **98**, 201408(R) (2018).

[62] Z. Xu, P. Ju, X. Gao, K. Shen, Z. Jacob, and T. Li, Observation and control of Casimir effects in a sphere-plate-sphere system, Nat. Commun. **13**, 6148 (2022).

[63] A. Milling, P. Mulvaney, and I. Larson, Direct measurement of repulsive van der Waals interactions using an Atomic Force Microscope, J. Colloid Interface Sci. **180**, 460 (1996).

[64] S.-w. Lee and W. M. Sigmund, AFM study of repulsive van der Waals forces between Teflon AF$^{TM}$ thin film and silica or alumina, Colloids Surf., A **204**, 43 (2002).

[65] A. A. Feiler, L. Bergström, and M. W. Rutland, Superlubricity using repulsive van der Waals forces, Langmuir **24**, 2274 (2008).

[66] J. N. Munday, F. Capasso, and V. A. Parsegian, Measured long-range repulsive Casimir-Lifshitz forces, Nature (London) **457**, 170 (2009).

[67] P. J. van Zwol and G. Palasantzas, Repulsive Casimir forces between solid materials with high-refractive-index intervening liquids, Phys. Rev. A **81**, 062502 (2010).

[68] R. F. Tabor, R. Manica, D. Y. C. Chan, F. Grieser, and R. R. Dagastine, Repulsive van der Waals forces in soft matter: Why bubbles do not stick to walls, Phys. Rev. Lett. **106**, 064501 (2011).

[69] M. Elbaum and M. Schick, Application of the theory of dispersion forces to the surface melting of ice, Phys. Rev. Lett. **66**, 1713 (1991).

[70] M. Dou, F. Lou, M. Boström, I. Brevik, and C. Persson, Casimir quantum levitation tuned by means of material

properties and geometries, Phys. Rev. B **89**, 201407(R) (2014).

[71] W. Kunz, *Specific Ion Effects* (World Scientific, Singapore, 2009).

[72] H. B. Chan, V. A. Aksyuk, R. N. Kleiman, D. J. Bishop, and F. Capasso, Quantum mechanical actuation of microelectromechanical systems by the Casimir force, Science **291**, 1941 (2001).

[73] F. W. DelRio, M. P. de Boer, J. A. Knapp, E. David Reedy, P. J. Clews, and M. L. Dunn, The role of van der Waals forces in adhesion of micromachined surfaces, Nat. Mater. **4**, 629 (2005).

[74] D. A. T. Somers, J. L. Garrett, K. J. Palm, and J. N. Munday, Measurement of the Casimir torque, Nature (London) **564**, 386 (2018).

[75] P. Thiyam, P. Parashar, K. V. Shajesh, O. I. Malyi, M. Boström, K. A. Milton, I. Brevik, and C. Persson, Distance-dependent sign reversal in the Casimir-Lifshitz torque, Phys. Rev. Lett. **120**, 131601 (2018).

[76] L. M. Woods, D. A. R. Dalvit, A. Tkatchenko, P. Rodriguez-Lopez, A. W. Rodriguez, and R. Podgornik, Materials perspective on Casimir and van der Waals interactions, Rev. Mod. Phys. **88**, 045003 (2016).